ILASS 2008
Sep. 8-10, 2008, Como Lake, Italy

Paper ID ILASS08-P-14

# EVALUATION OF FUEL SPRAY ATOMIZATION MODELS FOR CONDITIONS APPLICABLE TO LARGE MARINE DIESEL ENGINES

Christos Chryssakis, Lambros Kaiktsis

Dept. of Naval Architecture & Marine Engineering
National Technical University of Athens
Heroon Polytechniou 9, GR-15773 Zografou, Greece
Phone: +30-210-77211441, Fax: +30-210-7721117
cchryssa@naval.ntua.gr, kaiktsis@naval.ntua.gr

**ABSTRACT**

Due to the large size of marine diesel engines (an order of magnitude larger than automotive ones) it is expected that the physics of spray atomization, namely the primary and secondary breakup mechanisms, may differ from those encountered in the smaller automotive engines. Typically, diesel sprays in small engines disintegrate according to the shear and catastrophic breakup mechanisms. It is expected that, due to larger droplet sizes, injection velocities, and cylinder pressure, the catastrophic breakup mechanism will prevail in large marine diesel engines. The significant differences in the controlling non-dimensional parameters (Reynolds and Weber numbers) suggest that an evaluation of currently available atomization models for the conditions of large marine engines is necessary. In this work, we perform a preliminary evaluation of the most commonly used Lagrangian models for diesel sprays, namely the KH-RT, and E-TAB models, as well as the recently developed Unified Spray Breakup (USB) model. The problem setup consists of a constant-volume vessel, in which fuel injection is simulated with a KIVA-based CFD code. Here, tip penetration and breakup mechanisms are reported and compared for the three models of interest. Insight from experimental measurements is used to evaluate the computational results.

## INTRODUCTION

A major challenge with modelling fuel sprays for large marine diesel engines is related to the size of the orifice of the injector nozzle, which is an order of magnitude larger than the nozzles typically used in automotive applications. The difference in size strongly affects the Reynolds and Weber numbers of the emerging liquid jet, which control the primary and, subsequently, the secondary atomization mechanisms.

The atomization mechanisms are controlled by turbulence levels (depending on the Reynolds number), aerodynamic interactions between the liquid fuel and the surrounding air (triggering instabilities on the gas-liquid interface), and surface tension effects. The competing effects of aerodynamic forces and surface tension are expressed by the Weber number of the flow, which controls the atomization mechanism [1]. Typically, diesel sprays in small engines disintegrate according to the shear and catastrophic breakup mechanisms [2]. It is expected that, due to larger droplet sizes, injection velocities, and cylinder pressure, the catastrophic breakup mechanism will prevail in large marine diesel engines. Operating conditions in these engines correspond to injection pressures of the order of 1000 bar, injection velocities of the order of 500 m/s, and maximum cylinder pressures of the order of 150 bar [3]. The nozzle diameter is typically of the order of 1 mm, about an order of magnitude larger than in automotive applications. The resulting level of Reynolds (Re) and Weber (We) numbers of the spray jet is given in Table 1, and compared with typical values for automotive applications.

In this work, two commonly used Lagrangian models will be used, namely the E-TAB [4] and the KH-RT [5] models, as well as the Unified Spray Breakup (USB) model, recently developed by Chryssakis & Assanis [2].

**Table 1:** Typical values of Spray Reynolds and Weber numbers for Marine and Automotive applications.

| | **Marine** | **Automotive** |
|---|---|---|
| **Re** | 120,000 | 20,000 |
| **We** | 500,000 | 50,000 |

In the followings, a brief description of the three Lagrangian atomization models is given, accompanied by the description of the test cases and a grid sensitivity analysis. Typical characteristics of fuel sprays, namely the tip penetration and breakup mechanisms, are presented and comparisons between the models are performed. Insight from experimental measurements is used to evaluate the computational results.

## COMPUTATIONAL MODELS

The computational models under consideration in this work are the Enhanced - Taylor Analogy Breakup (E-TAB), Kelvin-Helmholtz - Rayleigh-Taylor (KH-RT) and the Unified Spray Breakup (USB) model. The first two models have been extensively used for diesel spray simulations in automotive applications, while the E-TAB has been used for marine spray applications as well [3, 6]. The computational platform is the code KIVA-3V [7] for the KH-RT and USB models, and KIVA-3 [8] for E-TAB.

### E-TAB Model

The E-TAB model reflects a cascade of droplet breakups, in which the breakup condition is determined by the Taylor

droplet oscillator dynamics. The droplet size is reduced until the product droplets reach a stable condition. The model maintains the droplet deformation dynamics of the TAB model [9]. According to this approach, the droplet distortion is described by a forced damped harmonic oscillator, in which the forcing term corresponds to the aerodynamic droplet-gas interaction, the damping is due to the liquid viscosity, and the restoring force is supplied by the surface tension.

Breakup occurs when the normalized droplet distortion, *y(t)*, exceeds the critical value of one. The rate of droplet creation is

$$\frac{d}{dt}m(t) = -3K_{br}m(t)$$

where *m(t)* is the mean mass of the product droplet distribution, and $K_{br}$ a constant that depends on the breakup regime (the bag and shear/stripping breakup regimes are considered). This correspondingly leads to an exponential relation between the product and parent droplet radius, *r* and $\alpha$:

$$\frac{r}{\alpha} = e^{-K_{br}t}$$

Droplets are initialized with a "negative" deformation velocity in order to avoid the almost immediate breakup of highly unstable initial ligaments and to extend their lifetime to levels comparable with experimentally observed jet breakup lengths.

**KH-RT Model**

The KH-RT model [5] accounts for two steps: primary and secondary breakup. The Kelvin-Helmholtz (KH) instability model is used to predict the primary breakup of the intact liquid core of the diesel jet, while the secondary breakup of individual drops is modelled with the KH model in conjunction with the Rayleigh-Taylor (RT) accelerative instability model.

The KH model postulates that a parent droplet with radius *r* breaks up to form new droplets with radius $r_c$, such that

$$R_c = B_o \Lambda_{KH}$$

where $\Lambda_{KH}$ is the wavelength corresponding to the wave with the maximum growth rate and $B_o$ a constant equal to 0.61. During breakup the parent droplet reduces in diameter due to the loss of mass. The rate of change of the radius of this droplet is calculated as:

$$\frac{dr}{dt} = \frac{r - r_c}{\tau_{KH}}$$

where $\tau_{KH}$ is the breakup time defined by:

$$\tau_{KH} = \frac{3.726 B_1 r}{\Omega_{KH} \Lambda_{KH}}.$$

The constant $B_1$ has originally been set equal to 4.7 in the present work, but can have a variety of values ranging from 1.73 to 60 [10].

The RT model is used in conjunction with the KH model to predict the secondary breakup of the droplets. The RT model predicts instabilities on the surface of the drop that grow until a certain characteristic breakup time is reached, when the drop finally breaks up.

**USB Model**

The fuel injection process has been divided in three subprocesses, namely, primary atomization, drop deformation and aerodynamic drag, and secondary atomization [2]. The primary atomization is modelled based on the Huh et al. approach [11]. The model considers the effects of both infinitesimal wave growth on the jet surface and jet turbulence including cavitation dynamics. Initial perturbations on the jet surface are induced by the turbulent fluctuations in the jet, originating from the shear stress along the nozzle wall and possible cavitation effects. This approach overcomes the inherent difficulty of wave growth models, where the exponential wave growth rate becomes zero at zero perturbation amplitude. The model is based on the following two main assumptions:

1. The integral length scale of turbulence is the dominant length scale of atomization,
2. The time scale of the atomization is the linear sum of the turbulence and wave growth time scales.

The drop deformation and secondary atomization have been modelled based on the physical properties of the system, independent of the way the droplets were created. The secondary atomization has been further divided into four breakup regimes, based on experimental observations reported in the literature [1]. The determination of the appropriate secondary atomization regime is based solely on the Weber number of the droplets. For low Weber numbers (less than 12) atomization does not occur and only droplet deformation takes place. For higher values of Weber number, the following regimes are considered:

- Bag breakup, 12<We<20
- Multimode breakup, 20<We<80
- Shear breakup, 80<We<800
- Catastrophic breakup, 800<We

The breakup times and resulting droplet sizes for each breakup regime are estimated based on experimentally verified correlations for each regime.

Once droplet secondary atomization has been completed, further disintegration (tertiary breakup) does not occur, and droplets are assumed to reach a stable condition.

**Test Cases**

The problem setup consists of a constant-volume chamber with dimensions 20cm×10cm×10cm. The chamber is filled with $N_2$, the pressure is maintained at 100 bar (10 MPa) and temperature at 300 K. The temperature has been kept low so that only the liquid atomization of the fuel jets is tested, without including the evaporation process. Two different nozzle diameters are tested, one representative of large, low-speed two-stroke diesel engines, and one corresponding to medium-speed marine engines, as shown in Table 2.

**Table 2:** Nozzle characteristics.

| | **Application** | **Diameter [mm]** |
|---|---|---|
| **Nozzle A** | Large, Low-Speed | 0.9 |
| **Nozzle B** | Medium-Speed | 0.37 |

The injection velocity profile for Nozzle A is representative of a typical velocity profile for a 2-stroke engine, as measured by Wärtsilä Switzerland [3] and is illustrated in Figure 1.

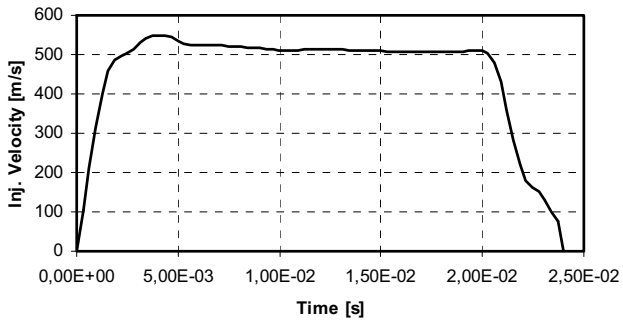


**Figure 1:** Injection velocity history for Nozzle A.

For Nozzle B, a simplified, constant injection rate has been used, with an injection velocity of 300 m/s, representative of injection in medium-speed marine engines [12].

### Grid Sensitivity Study

Grid sensitivity has been assessed by using three different grid resolutions in the injection direction. Namely, grid spacings of 1.5, 2.0, and 3.0 mm have been tested, and the spray tip penetrations have been compared, for Nozzle A, for each one of the breakup models. The results are shown in Figures 2, 3, and 4, for the E-TAB, KH-RT, and USB models respectively. Interestingly, the E-TAB model has negligible grid dependency, while the USB model is grid independent for Dz<2.0 mm. The KH-RT model is more grid-dependent and seems to converge for Dz=1.5 mm.

## RESULTS AND DISCUSSION

Observation of Figures 2-4 reveals significant differences in tip penetration predictions for the three models. The E-TAB predicts the lowest penetration, the USB the highest, and KH-RT lies in the middle. These differences can be attributed to the different assumptions and breakup mechanisms employed in each model.

The long penetration of the USB model is mainly due to the way that primary atomization is modelled. At relatively low speeds, encountered at the start of the injection, the liquid core does not break up easily and its momentum is maintained. Furthermore, it is assumed that its aerodynamic drag coefficient is equal to that of a cone ($C_D$=0.3), due to its cone-like shape. Therefore, deceleration is slow, leading to long penetration lengths. As injection velocities increase, primary atomization occurs very quickly, resulting in small drops that deform and disintegrate according to the secondary atomization mechanisms discussed above.

Experimental measurements are not available yet for this case, so the model predictions cannot be confirmed. However, it appears that the primary atomization mechanism of the USB model is partly correct: due to low injection velocities at the onset of the injection, the resulting liquid core breaks up slowly, yielding large droplets, and penetrating relatively deep into the ambient gas, according to Sallam and Faeth [13]. These droplets should disintegrate in later times, therefore resulting in lower tip penetration at later times. Implementing this mechanism in the model will likely allow predicting the changing of the slope of the tip penetration, observed often in experimental measurements of tip penetration [12].

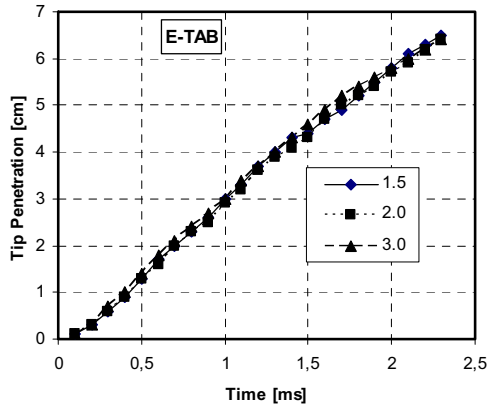


**Figure 2:** Results of Grid Sensitivity Analysis for the E-TAB model: spray penetration vs. time, for different sizes of computational cells.

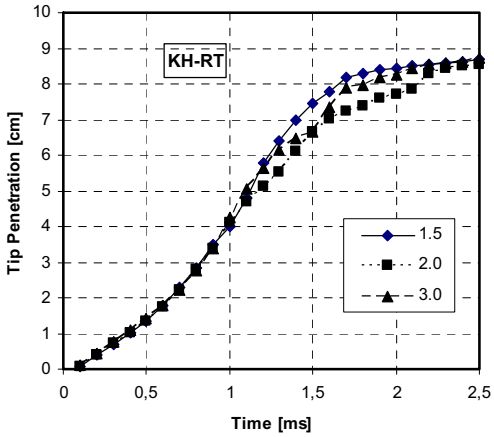


**Figure 3:** Results of Grid Sensitivity Analysis for the KH-RT model: spray penetration vs. time, for different sizes of computational cells.

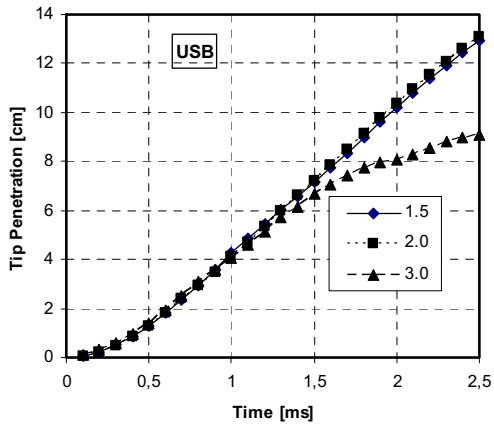


**Figure 4:** Results of Grid Sensitivity Analysis for the USB model: spray penetration vs. time, for different sizes of computational cells.

This explanation can only partly justify the large differences between the tip penetrations among the three models. Further research, supported by experimental measurements, is required for clarifying this issue.

The very low penetration of the KH-RT model is attributed to the coefficient $B_1$ that controls the breakup rate. Calibration

of this constant, based on experimental data, is necessary for correct predictions for each type of injector. One more value has been tested, $B_1$=10, and the tip penetration is significantly higher, closer to the USB model predictions, as shown in Figure 5.

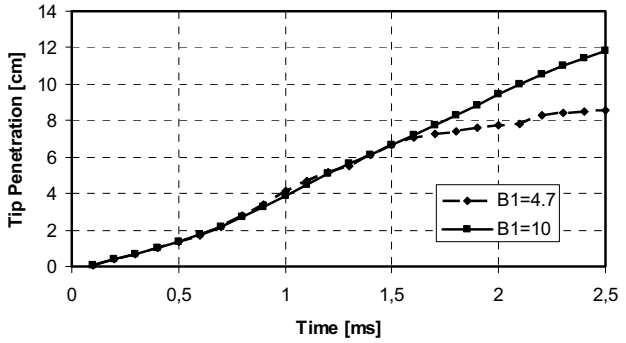


**Figure 5:** Tip Penetration Results for KH-RT, $B_1$=4.7 and 10.

### Injector Nozzle with $d_o$=0.37mm

A second series of computations has been performed with an injector nozzle diameter of $d_o$=0.37 mm, injection duration of 2.5ms, and injected mass of 68mg. The results for tip penetration are presented in Figure 6.

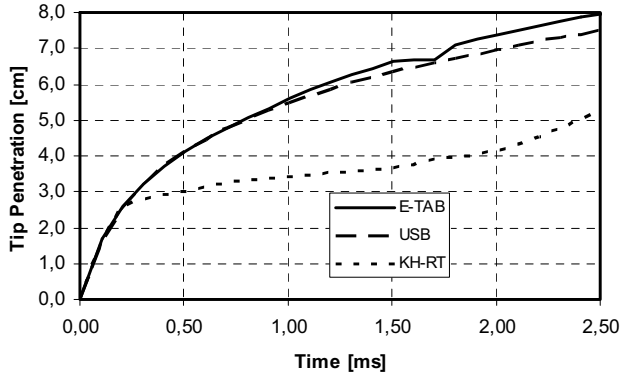


**Figure 6:** Tip Penetration Results for $d_o$=0.37, $U_{inj}$=300m/s.

In this case, tip penetration predictions with the USB and E-TAB models are nearly identical. We underline that the initial phase of the injection is not considered and only high velocities have been used. This observation indicates that the very high tip penetrations in the previous case for the USB model are indeed due to modelling of the primary atomization mechanism at low injection velocities. The E-TAB model has been previously tested for very similar conditions [11] and the results were reasonably close to experimental measurements.

As for the larger nozzle (A), the KH-RT predicted penetration lengths are significantly shorter, when $B_1$=4.7, due to model calibration reasons.

## CONCLUSIONS

In this work a preliminary comparison of three Lagrangian spray atomization models has been performed, for two different injector nozzles, representative of low- and medium-speed marine engines, respectively.

It is concluded that when a realistic injection velocity profile is used, the USB model can lead to very high tip penetration predictions, because it fails to handle correctly primary atomization at low injection velocities.

The KH-RT model depends strongly on calibration and has to be tuned for proper predictions of marine diesel sprays.

It is also interesting to explore the reasons that lead the E-TAB model to significantly lower predictions of tip penetration than the KH-RT and the USB models when large nozzle diameters are used.

## ACKNOWLEDGMENT

The authors acknowledge the financial support by a Marie-Curie International Reintegration Grant (IRG), Agreement Nr. 207232.

## REFERENCES

[1] Faeth, G.M., Hsiang, L.-P., Wu, P.-K., Structure and Breakup Properties of Sprays, *International Journal of Multiphase Flow,* Vol. 21, Suppl. pp. 99-127, 1995.

[2] Chryssakis, C., Assanis, D.N., A Unified Fuel Spray Breakup Model for Internal Combustion Engine Applications, *Atomization and Sprays*, Vol. 18, No. 5, pp. 375-426, 2008.

[3] Kontoulis, P., Chryssakis, C., Kaiktsis, L. Evaluation of Pilot Injections in a Large Two-Stroke Marine Diesel Engine, Using CFD and T-φ Mapping, *COMODIA 2008*, Sapporo, Japan, July 2008.

[4] Tanner, F.X., Liquid Jet Atomization and Droplet Breakup Modeling of Non-Evaporating Diesel Fuel Sprays, *SAE Technical Paper* 970050, 1997.

[5] Beale, J.C., Reitz, R.D., Modeling Spray Atomization with the Kelvin-Helmholtz/Rayleigh-Taylor Hybrid Model, *Atomization and Sprays*, vol. 9, pp. 623-650, 1999.

[6] Tanner, F.X., Weisser, G., Simulation of Liquid Jet Atomization for Fuel Sprays by Means of a Cascade Drop Breakup Model, *SAE Technical Paper* 980808, 1998.

[7] Amsden A.A., KIVA-3V: A Block-Structured KIVA Program for Engines with Vertical or Canted Valves, Los Alamos National Laboratory LA-13313-MS, July 1997

[8] Amsden, A.A., KIVA-3: A KIVA Program with Block-Structured Mesh for Complex Geometries, Los Alamos National Laboratory LA-12503-MS, 1993

[9] O'Rourke, P.J., Amsden, A.A., The TAB method for numerical calculation of spray droplet breakup, *SAE Technical Paper* 872089, 1987.

[10] Patterson, M.A., Reitz, R.D., Modeling the Effects of Fuel Spray Characteristics on Diesel Engine Combustion and Emissions, *SAE Technical Paper* 980131, 1998

[11] Huh, K.Y. Lee, E. Koo, J.-Y., Diesel Spray Atomization Model Considering Nozzle Exit Turbulence Conditions, *Atomization and Sprays*, vol. 8, pp. 453–469, 1998

[12] Larmi, M., Rantanen, P., Tiainen J., Kiijarvi, J., Tanner, F.X., Stalsberg-Zarling, K., Simulation of Non-Evaporating Diesel Sprays and Verification with Experimental Data, *SAE Technical Paper* 2002-01-0946

[13] Sallam, K.A., Faeth, G.M., "Surface Properties During Primary Breakup of Turbulent Liquid Jets in Still Air", *AIAA Journal*, Vol. 41, No. 8, pp. 1514-1524, 2003